Received: 15 March 2023 | Revised: 26 July 2023 | Accepted: 2 August 2023

DOI: 10.1111/cas.15934

Cancer Science WILEY

ORIGINAL ARTICLE

Promotion of squamous cell carcinoma tumorigenesis by oncogene-mediated THG-1/TSC22D4 phosphorylation

Nohara Goto[1,2] | Hiroyuki Suzuki[1,3] | Ling Zheng[1] | Yasuhito Okano[1] | Yukari Okita[1] | Yukihide Watanabe[1] | Yukinari Kato[3] | Mitsuyasu Kato[1]

[1]Department of Experimental Pathology, Faculty of Medicine, University of Tsukuba, Tsukuba, Japan

[2]Ph.D. Program in Human Biology, School of Integrative and Global Majors, University of Tsukuba, Tsukuba, Japan

[3]Department of Antibody Drug Development, Tohoku University Graduate School of Medicine, Sendai, Japan

Correspondence
Hiroyuki Suzuki, Department of Antibody Drug Development, Tohoku University Graduate School of Medicine, 2-1 Seiryo-machi, Aoba-ku, Sendai, Miyagi 980-8575, Japan.
Email: hiroyuki.suzuki.b4@tohoku.ac.jp

Mitsuyasu Kato, Department of Experimental Pathology, Faculty of Medicine, University of Tsukuba, 1-1-1 Tennoudai, Tsukuba, Ibaraki 305-8575, Japan.
Email: mit-kato@md.tsukuba.ac.jp

Funding information
Japan Society for the Promotion of Science, Grant/Award Number: 17K19580, 25640059, 22K06995, 19K07473, 16K08706, 22K15596 and 20K16434

Abstract

Carcinoma cells possess high proliferative and invasive potentials and exhibit a resilience against stresses, metabolic disorder, and therapeutic efforts. These properties are mainly acquired by genetic alterations including driver gene mutations. However, the detailed molecular mechanisms have not been fully elucidated. Here, we provide a novel mechanism connecting oncogenic signaling and the tumorigenic properties by a transforming growth factor-β1-stimulated clone 22 (TSC-22) family protein, THG-1 (also called as TSC22D4). THG-1 is localized at the basal layer of normal squamous epithelium and overexpressed in squamous cell carcinomas (SCCs). THG-1 knockdown suppressed SCC cell proliferation, invasiveness, and xenograft tumor formation. In contrast, THG-1 overexpression promoted the EGF-induced proliferation and stratified epithelium formation. Furthermore, THG-1 is phosphorylated by the receptor tyrosine kinase (RTK)-RAS-ERK pathway, which promoted the oncogene-mediated tumorigenesis. Moreover, THG-1 involves in the alternative splicing of CD44 variants, a regulator of invasiveness, stemness, and oxidative stress resistance under the RTK pathway. These findings highlight the pivotal roles of THG-1 as a novel effector of SCC tumorigenesis, and the detection of THG-1 phosphorylation by our established specific antibody could contribute to cancer diagnosis and therapy.

KEYWORDS
CD44, monoclonal antibody, phosphorylation, receptor tyrosine kinase, squamous cell carcinoma, THG-1, TSC22D4

1 | INTRODUCTION

Protection against physical and chemical insults, infection, and water loss is provided by the stratified squamous epithelium.[1,2] Squamous cell carcinomas (SCCs) arise from epithelial tissues that can be classified as stratified squamous epithelium including skin,[3] esophagus,[4] cervix,[5] head and neck[6] and nonsquamous epithelia including the lung airway epithelium.[7] Despite advances of treatment in recent

Abbreviations: CD44s, CD44 standard; CD44v, CD44 variants; EGFR, epidermal growth factor receptor; FGFR, fibroblast growth factor receptor; GSH, reduced glutathione; HB-EGF, heparin-binding epidermal growth factor-like growth factor; IHC, immunohistochemistry; mAb, monoclonal antibody; NOD-Scid, NOD.CB17-*Prkdc*^{scid}/NCrCrl; PI3K, phosphatidylinositol-3 kinase; ROS, reactive oxygen species; RTK, receptor tyrosine kinase; SAM68, Src-associated in mitosis 68 kDa protein; SCC, squamous cell carcinoma; SD, standard deviation; TSC-22, transforming growth factor-β1-stimulated clone 22; xCT, cystine–glutamate transporter.

years, SCC survival has not been improved significantly.[8] Further understanding of the molecular mechanisms underlying SCC progression is a prerequisite for improving patient therapy and prognosis.

Genomic and molecular characterization of SCC including lung, esophagus, head and neck, and skin SCCs have been studied to understand the molecular characteristics and driver gene mutations.[9] Comprehensive genomic characterization of 178 lung SCC revealed that broad range of receptor tyrosine kinase (RTK) upregulation by the genomic alteration of epidermal growth factor receptor (EGFR) and fibroblast growth factor receptor (FGFR) families were observed in 26% of tumors. The activation of the RAS-BRAF pathway was observed in 24% of tumors. Furthermore, one of the components of the phosphatidylinositol 3-kinase (PI3K)/AKT pathway was altered in 47% of tumors, and the alterations in the PI3K/AKT pathway genes were mutually exclusive with EGFR alterations.[10] The dependence of lung SCC on these individual alterations remains to be defined functionally, and the identification of the substrate which determines the characteristics of SCC is also important. Although molecular targeting therapies for lung adenocarcinoma against EGFR, BRAF, HER2, $KRAS^{G12C}$, and ALK fusions have been successful,[11] activating mutations in EGFR and ALK fusions are typically not observed in lung SCC. Therefore, targeted agents developed for lung adenocarcinoma are largely ineffective against lung SCC.

The outcome of esophageal SCC has remained unchanged during the last several decades, with a 5-year survival rate ranging from 15% to 20%.[8] The driver gene mutations were also revealed by a large scale of whole-exome or targeted deep sequencing. The mitogen-activated protein kinase and PI3K pathways are augmented by multiple mechanisms including the amplification and overexpression of RTKs and the activating mutations KRAS and PIK3CA.[12] Although the driver gene mutations were revealed in SCC, the substrates which determine the property of SCC have not been fully elucidated.

CD44 is a cell surface glycoprotein and known as a major receptor for hyaluronic acid, which is involved in tumor cell adhesion, migration, and invasiveness.[13] CD44 is involved in cancer stem cell properties, epithelial to mesenchymal transition, and a resistance to chemo- and radiotherapy.[14] The CD44 gene consists of multiple exons in humans. The first five (1–5) and the last five (16–20) exons produce CD44 standard form (CD44s). The variant exons can be alternatively spliced and assembled with exons contained in CD44s and are referred to as CD44 variants (CD44v).[15] The CD44v provides binding site for cytokines and growth factors. For instance, CD44v3–10 functions as a coreceptor of RTKs by binding to FGFs and heparin-binding epidermal growth factor-like growth factor (HB-EGF) via the v3-encoded region[16] and hepatocyte growth factor receptor via the v6-encoded region.[17] Furthermore, CD44v interacts with a subunit of cystine–glutamate transporter (xCT) via the v8–10-encoded region and confers oxidative stress resistance in several carcinomas.[18] Therefore, CD44v is a promising target for cancer diagnosis and therapy. Therefore, understanding the molecular mechanism of CD44v processing is important for targeting CD44 in cancer therapy.[19]

Transforming growth factor-β1-stimulated clone 22 (TSC-22) was identified as a TGF-β1 target gene[20] and possesses growth-suppressive function.[21] TSC-22 (TSC22D1) and related family members, including KIAA0669/TSC22D2, GILZ/TSC22D3, and THG-1/TSC22D4 share a conserved Tsc-box and leucine zipper domains.[22] Among them, THG-1 was originally identified as a TSC-22-interacting protein[23]; however, the physiological and/or pathological functions of THG-1 have not been elucidated. In this study, we show that THG-1 is expressed in normal squamous epithelium and overexpressed in SCCs. THG-1 is phosphorylated by receptor tyrosine kinase pathways, which is important for the tumorigenic potential of THG-1. Furthermore, THG-1 and its phosphorylation promote the production of CD44v. These results indicated that THG-1 is involved in the tumorigenesis of SCC under the RTK signaling pathway.

2 | MATERIALS AND METHODS

2.1 | Cell lines

HEK293T and P3X63Ag8U.1 (P3U1) cells were purchased from the American Type Culture Collection (ATCC). HaCaT cells were provided by Dr. N.E. Fusenig (DKFZ). The TE series of esophageal tumor cell lines were obtained from the Cell Resource Center for Biomedical Research, Institute of Development, Aging and Cancer, Tohoku University. The KYSE series of esophageal tumor cell lines were purchased from the Japanese Collection of Research Bioresources Cell Bank. Human dermal fibroblasts were obtained from RIKEN BioResource Research Center (BRC). These cells were cultured in Dulbecco's modified Eagle's medium (DMEM, Sigma-Aldrich) supplemented with 10% fetal bovine serum (FBS) and 50 U/mL penicillin and 50 μg/mL streptomycin (FUJIFILM Wako Pure Chemical). P3X63Ag8U.1 (P3U1) cells were obtained from ATCC and cultured in RPMI1640 medium (Sigma-Aldrich) with 10% FBS. EGF was obtained from Sigma-Aldrich.

2.2 | Antibodies

THG-1 (4G7, Abnova); FLAG epitope tag (M2, Sigma-Aldrich); HA epitope tag (3F10, Roche Diagnostics); β-actin (Sigma-Aldrich); E-Cadherin (610,181, BD Bioscience); Phospho-EGFR ($pTyr^{1068}$, C04301, Abcam); EGFR (sc-101, Santa Cruz); Phospho-ERK1/2 ($pThr^{202}/pTyr^{204}$, #9106, Cell Signaling); ERK1/2 (#9102, Cell Signaling) or ERK2 (sc-154, Santa Cruz); Phospho-Akt (pS^{473}, #9271, Cell Signaling); Akt (#9272, Cell Signaling); c-Myc (sc-764, Santa Cruz); JunB (sc-8051, Santa Cruz); Ki67 (Leica); pan-CD44-PE (Sigma-Aldrich); CD44v3 (3G5, for immunohistochemistry [IHC], R&D Systems, Inc.); CD44v3 (C_{44}Mab-6[24] for flow cytometry); CD44v9 (RV3, Cosmo Bio and C_{44}Mab-1[25]).

For generation of anti-phospho-THG-1(pS^{264}) antibody, BALB/c mice (CLEA) were immunized with injections of synthetic peptide PLDSRPS(pS)PALYFT (pTHG-1 peptide) plus C-terminal cysteine conjugated with the keyhole limpet hemocyanin at the C-terminus

(Eurofins Genomics KK). The spleen cells were fused with mouse myeloma P3U1 cells using a Sendai virus envelope, GenomONE-CF (Ishihara Sangyo).[26] Supernatants were subsequently screened using enzyme-linked immunosorbent assay which reacted with pTHG-1 peptide but not non-phospho-THG-1 peptide (PLDSRPSSPALYFT). From the positive wells, hybridomas were cloned by limiting dilution. Clone 18 could be applied to the immunoblot analysis, and clone 21 could be applied to immunofluorescence and IHC. Anti-THG-1 rabbit serum was obtained by the immunization of peptide (human THG-1 amino acid 176–193: PTSPGPQARSFTGGLGQL plus C-terminal cysteine) (Sigma-Aldrich). The rabbit serum was affinity-purified using the SulfoLink immobilization kit (Thermo Fisher Scientific).

2.3 | DNA constructs and transfection

cDNAs of TSC-22, GILZ, THG-1, HRas, and CD44v3–10 were cloned by polymerase chain reaction (PCR) and cloned into pcDNA, pcDEF3, pPyCAG-IB (provided by Dr. Niwa), and pCAG-IP[27] vectors. The THG-1 and HRas mutants were generated using a PCR-based method. cDNA of KIAA0669 was obtained from RIKEN BRC. cDNAs of constitutively active form of ERK2 (L73P/S151D) were provided by Dr. Fukamizu.[28] These constructs were transfected into cells by FuGENE6 (Roche Diagnostics). HaCaT cells stably expressing FLAG-THG-1 (WT and mutants) and HA-HRas^{G12V} were selected and maintained in the presence of 1 μg/mL of puromycin (Sigma-Aldrich) and 4 μg/mL of Blasticidin S (FUJIFILM Wako Pure Chemical).

2.4 | RNAi

RNAi-mediated knockdown of THG-1 was performed by using the pSUPER RNAi system (OligoEngine) and pLKO.1 (for lentivirus, Addgene). The 19-bp targeting sequence was 5'-GGACGTGTGTGGATGTTTA-3′ for shTHG-1#2,

5'-GAAGCCTGGTTGGCATTGA3' for shTHG-1#3,
5'-CCATCAGTGGTCACCTAGA-3′ for shTHG-1#4,
and 5'-GCGCGCTTTGTAGGATTCG-3′ for the nontargeting control. TE13 cells transfected with pSUPER.puro-shTHG-1#2, pSUPER.puro-shTHG-1#3, and pSUPER.puro-control were selected and maintained in the presence of 1 μg/mL of puromycin. For lentivirus-mediated THG-1 knockdown, control, #2, and #4 sequences were cloned into pLKO.1, and the lentiviruses were generated in HEK293T cells.

TE13 shTHG-1#2 cells were transfected with pcDNA3 or pcDNA3-CD44v3–10 vectors, and stable cell lines were generated in the presence of 0.8 mg/mL of G418 (Nacalai Tesque, Inc.).

2.5 | Tumor xenograft formation in mice

For the xenografts of TE13 cells, 1×10^7 cells were subcutaneously inoculated into NOD.CB17-*Prkdc*^{scid}/NCrCrl (NOD-Scid) mice (Charles River) with Matrigel (BD Biosciences). For the xenografts of the HaCaT-HRas^{G12V} cells, 5×10^6 cells were subcutaneously inoculated into female BALB/cAJcl-*nu*/*nu* mice (nude mice) (CLEA). After 60 days (TE13 cells) and 45 days (HaCaT-HRas^{G12V} cells), the tumor volumes were approximated using the following equation: volume $=(a\times b^2)\ \pi/6$, where a and b are the lengths of the major and the minor axes, respectively. Tumors were fixed and embedded in paraffin, and the sections were stained with indicated antibodies.

2.6 | Immunohistochemistry

The paraffin-embedded tissues were sectioned at 2- to 5-μm thickness, deparaffinized in xylene, rehydrated in graded ethanol solution, and immersed in citrate-NaOH buffer (10 mM sodium citrate, pH 6.0) for 20 min at 115°C, 121 kPa. After blocking with SuperBlock T20 (Thermo Fisher Scientific, Inc.), sections were incubated with anti-THG-1 (4G7), phospho-THG-1(pS^{264}) (clone 21), Ki67, and CD44v9 (RV3) overnight at 4°C and then treated with the EnVision+ kit for mouse (Agilent Technologies Inc.) or Histofine reagent for rat IgG (Nichirei biosciences, Inc.) for 30 min. Color was developed using 3,3′-diaminobenzidine tetrahydrochloride (DAB; Agilent Technologies Inc.). Counterstaining was performed with hematoxylin (FUJIFILM Wako Pure Chemical Corporation).

2.7 | Specimens and tissue microarrays

Tissue microarrays of tumors of the esophagus (124 cases: 121 SCCs and 3 adenocarcinomas), the lung (114 cases: 34 SCCs, 58 adenocarcinomas, 10 large cell carcinomas, and 12 small cell carcinomas), the cervix uteri (120 SCCs, 8 adenosquamous carcinomas and 10 adenocarcinomas), and the stomach (20 cases: 1 SCC and 19 adenocarcinomas) were obtained from Cybrdi.

2.8 | Semiquantitative RT-PCR

Total RNA was isolated using Isogen (Nippon Gene), and cDNA was synthesized from PrimeScript RT Master Mix (TaKaRa). Semiquantitative PCR was performed using TaKaRa Ex taq (TaKaRa). The PCR primers to amplify both CD44s and CD44v,[18] and β-actin[21] were described previously.

2.9 | Statistical analysis

All data are expressed as mean ± standard deviation (SD). Statistical analysis was conducted with ANOVA and Sidak's multiple comparisons test. All calculations were performed using GraphPad Prism 8 (GraphPad Software, Inc.). A p-value of <0.05 was considered statistically significant.

Other methods of protein-based assay (immunoblot analysis and dephosphorylation assay), cell-based assays (cell proliferation assay, three-dimensional [3D] culture assay, sphere formation assay, immunofluorescence, and flow cytometry), and the supplemental figures are available in the supplemental materials and methods in Appendix S1.

3 | RESULTS

3.1 | Distribution of THG-1 in normal and carcinoma tissues

To investigate the roles and functions of THG-1, we examined the tissue distribution by IHC. Using a specific anti-THG-1 antibody (Figure S1A), we found that THG-1 was localized in the basal layer of stratified squamous epithelium including the forestomach, skin, and hair follicle epithelium of mice (Figure S1B). We next investigated THG-1 expression in human squamous epithelium and SCCs. THG-1 is localized in the basal layer of normal esophagus and uterine cervix mucosa, and diffuse expression of THG-1 was observed in esophageal SCC (positive THG-1 expression in 112 of 121 specimens [92.6%]) and cervical SCC (positive THG-1 expression in 96 of 120 specimens [80%]) (Figure 1A). Moreover, THG-1 expression was observed in lung SCC (23 of 34 specimens [67.6%]), but not in normal lung epithelium, adenocarcinoma, and small cell carcinoma (Figure 1B). THG-1 was sporadically expressed in large cell lung carcinoma (Figure 1B). Furthermore, THG-1 expression was observed in gastric SCC, but not adenocarcinoma (Figure 1C). THG-1 was mainly distributed in the cytoplasm and/or accumulated on cell–cell contact sites.

3.2 | Tumorigenic functions of THG-1

To investigate the function of THG-1 in SCC, we established THG-1-knockdown cells using two independent shRNAs (#2 and #3) in esophageal SCC cell line TE13 cells (Figure 2A). We first found that cell proliferation was reduced in THG-1-knockdown cells (Figure 2B). THG-1 knockdown also inhibited cell proliferation in five out of six human esophageal SCC cell lines (Figure S2). We

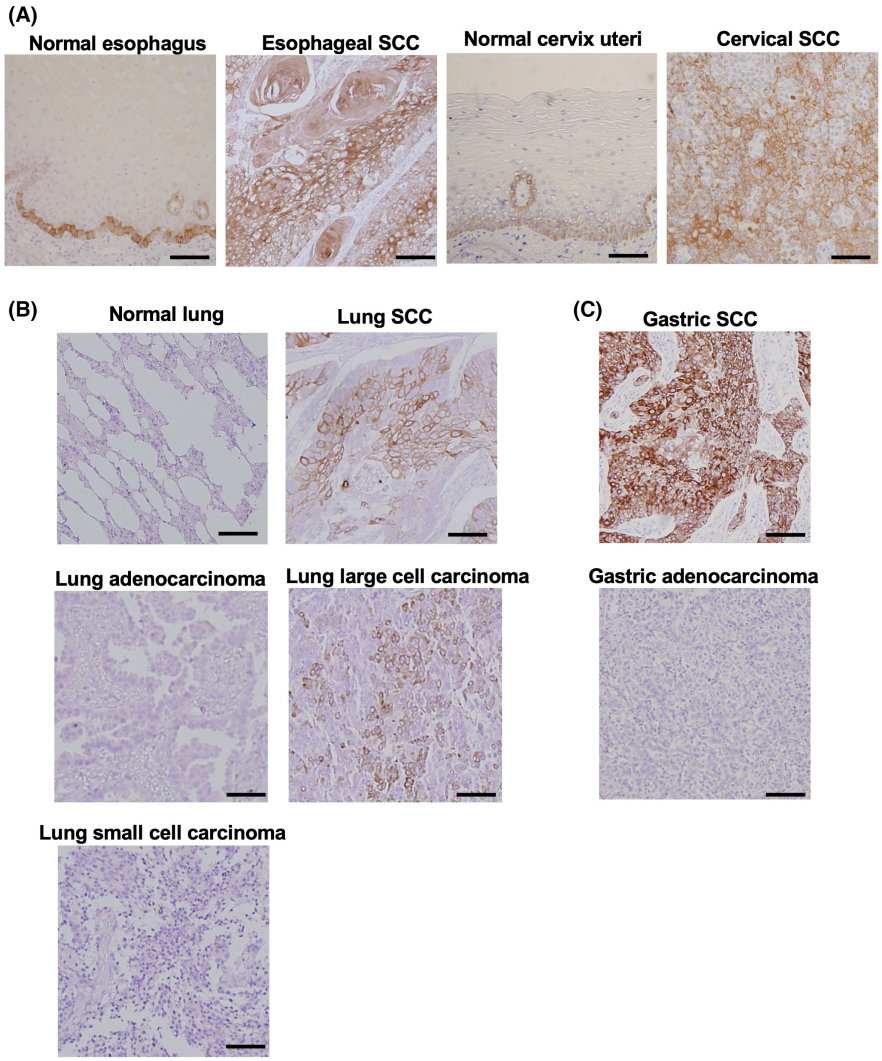

FIGURE 1 Distribution of THG-1 in normal stratified epithelium and squamous cell carcinomas (SCCs). (A) Immunohistochemistry of THG-1 in normal esophagus, esophageal SCC, normal cervix uteri, and cervical SCC. (B) Immunohistochemistry of THG-1 in normal lung and lung SCC, adenocarcinoma, large cell carcinoma, and small cell carcinoma. (C) Immunohistochemistry of THG-1 in gastric SCC and adenocarcinoma. Scale bars: 100 μm.

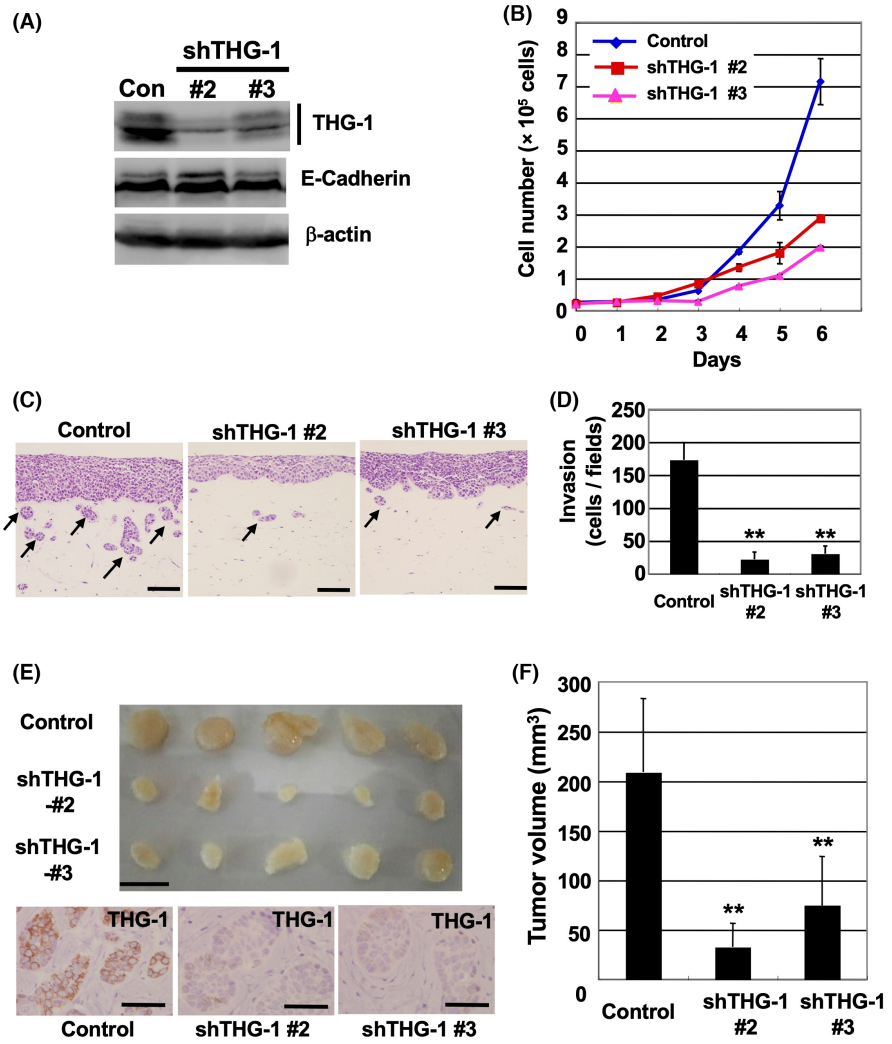

FIGURE 2 Functions of THG-1 in cell invasiveness and tumorigenicity. (A) Anti-THG-1, E-Cadherin, and β-Actin immunoblot analyses of TE13 cells expressing shRNAs targeting THG-1 (shTHG-1#2 and shTHG-1#3) or control shRNA. (B) Effect of THG-1 knockdown on cell proliferation. Error bars represent means ± SDs. (C, D) Effect of THG-1 knockdown on cell invasion into the collagen gels in 3D culture assay. Scale bars: 50 μm. Error bars represent means ± SDs. $^{**}p < 0.01$. (E, F) Effect of THG-1 knockdown on tumor formation in NOD-Scid mice (scale bar: 1 cm). Error bars represent means ± SDs. $^{**}p < 0.01$. Immunohistochemistry of THG-1 in xenograft tumors of TE13 cells (control, shTHG-1#2, and shTHG-1#3) (scale bars: 50 μm).

next investigated the THG-1 function using a 3D culture assay, in which air exposure promotes the stratification of SCC cells on the collagen gel as well as the invasion into the gels in the presence of EGF.[29] The invasion of TE13 cells into the gels was significantly reduced in THG-1-knockdown cells (Figure 2C,D). Finally, we investigated the role of THG-1 in tumor formation in NOD-Scid mice. As shown in Figure 2E,F, the tumor-forming ability was significantly reduced by THG-1 knockdown. These results indicated that THG-1 is overexpressed in SCC and has critical roles in tumorigenic ability.

3.3 | Effect of THG-1 in EGF-mediated proliferation and stratified epithelium formation

We examined the effect of overexpression of THG-1 in human keratinocyte HaCaT cells (Figure 3A). When the cells were cultured in the presence of EGF in 0.1% FBS condition, the HaCaT-THG-1 cells (clones 3 and 7) formed foci and showed increased cell proliferation compared with the mock-transfected control cells (Figure 3B). We next investigated the effect of THG-1 on the formation of stratified epithelium as shown in Figure 2C. Control cells formed stratified epidermoid structure, and differentiated flattened cells were observed on the surface. However, the differentiated cells were not observed on the surface of the HaCaT-THG-1 cells (Figure 3C). Furthermore, the proliferation marker Ki67-positive cells was increased from 13% to 60% with spreading over two-thirds of the layers of the THG-1-transfected epithelium (Figure 3D).EGF-induced cell migration and invasion were observed in TE13 cells, which were suppressed by THG-1 knockdown (Figure S3A,B). These results indicated that overexpression of THG-1 promotes EGF-induced proliferation and inhibits differentiation during the stratified epithelium formation.

3.4 | Phosphorylation of THG-1 by the RTK pathway

We next investigated the effect of THG-1 on EGF signaling using HaCaT-THG-1 cells. As shown in Figure S4A, THG-1 overexpression did not affect EGF signaling including EGF-induced phosphorylation of EGFR, ERK, and Akt and the induction of JunB and c-Myc. However, slowly migrated bands of THG-1 were induced by EGF, suggesting that EGF

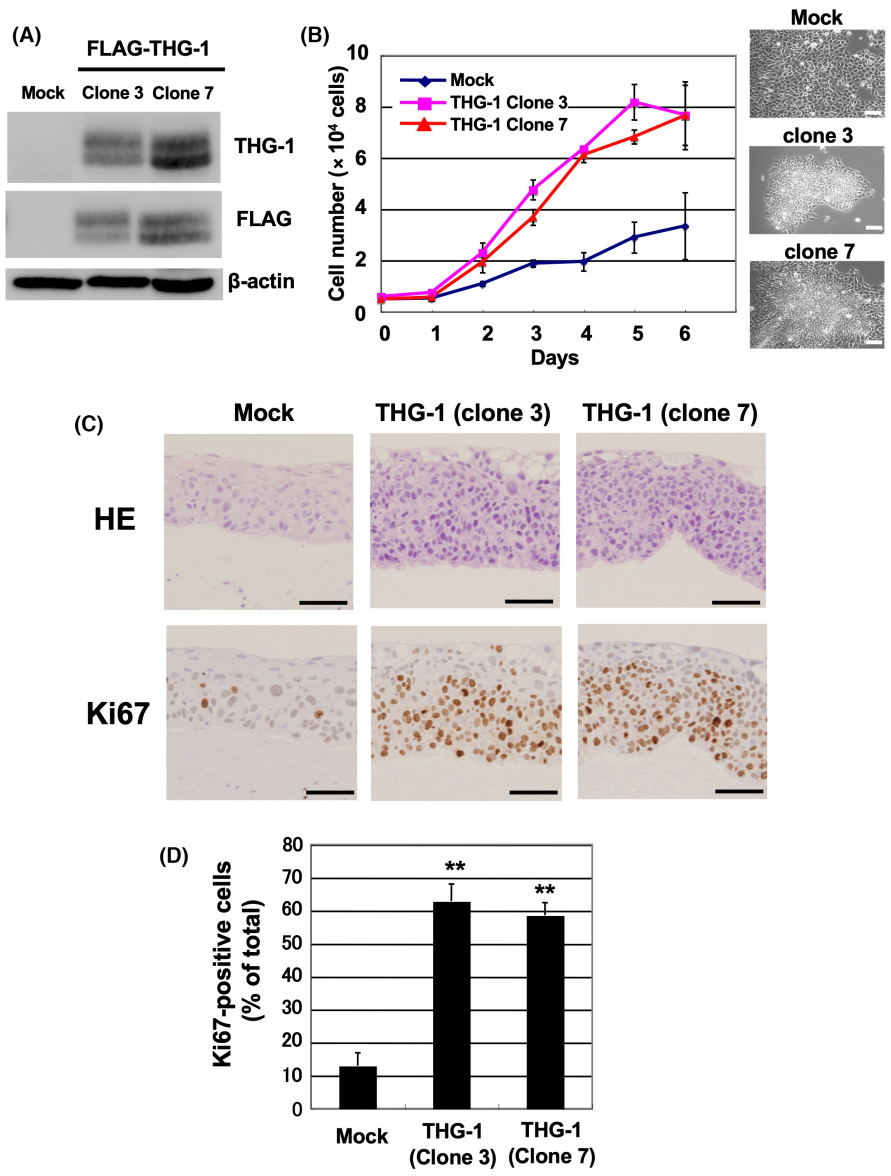

FIGURE 3 Effect of THG-1 in epidermal growth factor (EGF)-induced proliferation and stratified epithelium formation. (A) Anti-THG-1, FLAG, and β-Actin immunoblot analyses of HaCaT cells expressing FLAG-THG-1 (clone 3 and clone 7) or control (mock). (B) Effect of THG-1 on cellular proliferation and morphology in the presence of 50 ng/mL of EGF (in 0.1% FBS). Error bars represent means ± SDs. (C) Effect of THG-1 on the formation of stratified epithelium on collagen gels in 3D culture assay. Morphology of stratified epithelium in control and THG-1-transfected HaCaT cells. Sections were stained with anti-Ki67 antibody, and Ki67-positive cells were counted (D). $^{**}p < 0.01$. Error bars represent means ± SDs. Scale bars: 50 μm.

signaling modifies THG-1 in a post-translational manner. To confirm the nature of the slowly shifted THG-1, we treated the immunoprecipitated THG-1 with lambda protein phosphatase. As a result, the EGF-induced slowly shifted THG-1 was completely eliminated (Figure 4A), indicating that THG-1 is phosphorylated by EGF. The phosphorylation of THG-1 was inhibited by AG1478 (an EGFR inhibitor) and PD98059 (a MEK inhibitor), but not by LY294002 (a PI3 kinase inhibitor) (Figure S4B). THG-1 phosphorylation was also induced in THG-1 cotransfected with constitutively active $HRas^{G12V}$ (Figure 4B). Furthermore, THG-1 phosphorylation was also induced by the constitutively active form of ERK2 (L73P/S151D), but not by that of Akt (myr Akt) (Figure S4C).

To identify the phosphorylation site(s) of THG-1, we focused on the conserved P-X-S/T-P sequence, which is known to be phosphorylated by ERK,[30] and found that S^{264} corresponds to the ERK consensus sequence (Figure S5A). Therefore, we transfected the THG-1 (WT) and THG-1 (S264A) constructs into cells and stimulated them with EGF. As shown in Figure 4C, THG-1 (S264A) was not phosphorylated by EGF. Similar results were obtained by cotransfection with constitutively active $HRas^{G12V}$ and ERK2 (L73P/S151D) (Figure S5B,C), suggesting that THG-1 S^{264} is one of the important amino acids to be phosphorylated by the EGF-Ras-ERK pathway. We next established monoclonal antibodies (mAbs) which recognize phosphorylated THG-1 (pS^{264}). An anti-phospho-THG-1(pS^{264}) mAb (clone 18) recognized only the slowly migrated form of THG-1 in the presence of $HRas^{G12V}$ and ERK2 (L73P/S151D) (Figure S6A), and in EGF-treated HaCaT-THG-1 cells (Figure S6B). Furthermore, the antibody also recognized the endogenously phosphorylated THG-1 in the presence of EGF (Figure 4D). In immunofluorescence analysis (Figure 4E), THG-1 was detected diffusely in the cytoplasm in the absence of EGF. EGF stimulation changed the localization of THG-1 at the ruffling membranes. Another anti-phospho-THG-1(pS^{264}) mAb (clone 21) could detect phosphorylated THG-1 in both cytoplasm and ruffling membranes only in the presence of EGF. Finally, we stained the esophageal SCC sections with the anti-phospho-THG-1 (pS^{264}) antibody (clone 21) and found that the THG-1 phosphorylation was detected in those tumors (Figure 4F).

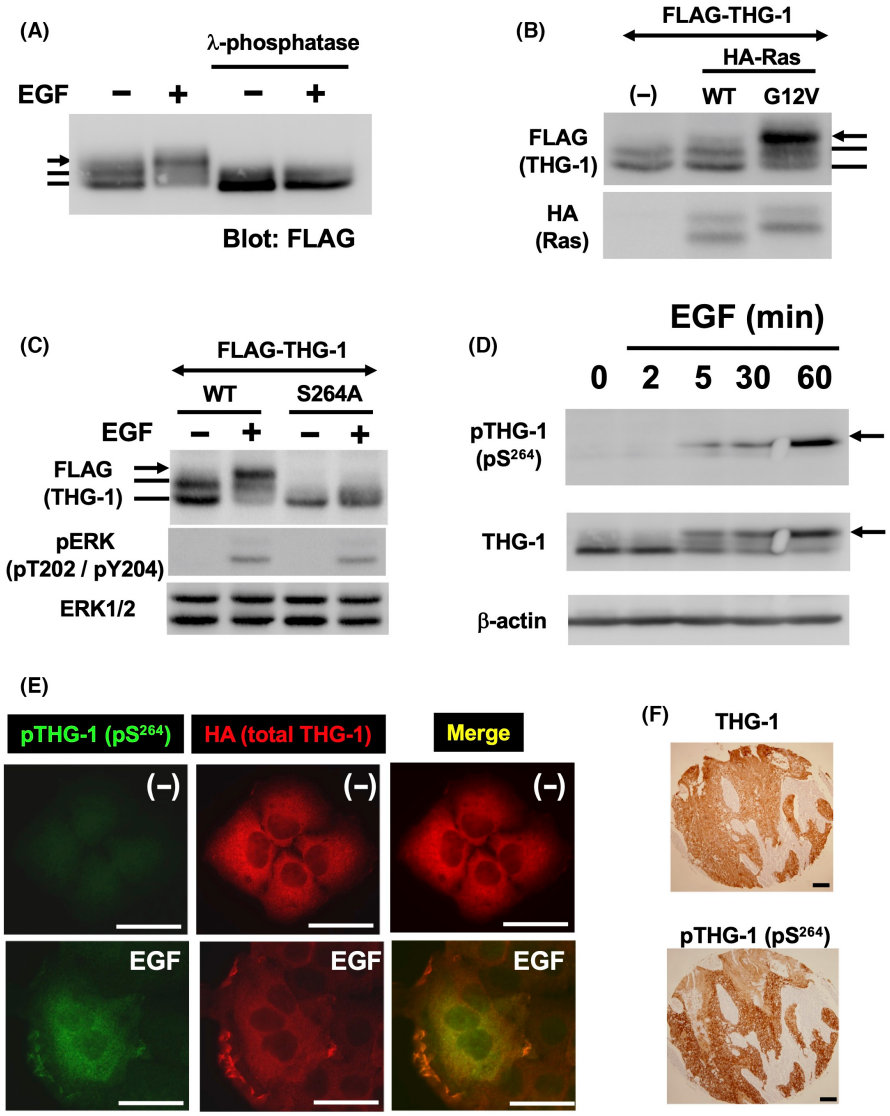

FIGURE 4 Phosphorylation of THG-1 by the epidermal growth factor (EGF)-RAS-ERK pathway. (A) Phosphorylation of THG-1 by EGF. HaCaT-FLAG-THG-1 cells were treated with EGF. Immunoprecipitated THG-1 was incubated with or without lambda protein phosphatase. Immunoblot analysis was performed using anti-FLAG antibody. The arrow indicates the phosphorylated THG-1. (B) THG-1 is phosphorylated by constitutively active $HRas^{G12V}$, but not by wild type (WT). HEK293T cells were transfected with FLAG-THG-1 with $HRas^{WT}$ and $HRas^{G12V}$. Immunoblot analysis was performed using anti-FLAG and HA antibodies. (C) S^{264} is an essential phosphorylation site of THG-1. HEK293T cells were transfected with FLAG-THG-1 (WT and S264A). The cells were treated with 50 ng/mL of EGF, and immunoblot analysis was performed using anti-FLAG, pERK, and ERK1/2 antibodies. (D) Using anti-phospho-THG-1(pS^{264}) mAb (clone 18), phosphorylated THG-1 was detected by immunoblot analysis in TE13 cells. (E) The phosphorylation of THG-1 was detected by immunofluorescence in HaCaT-HA-THG-1 cells (scale bars: 20 μm) using anti-phospho-THG-1(pS^{264}) mAb (clone 21). Anti-HA antibody detected HA-THG-1. (F) The phosphorylation of THG-1 was detected by immunohistochemistry in esophageal SCC using anti-phospho-THG-1(pS^{264}) mAb (clone 21) and anti-THG-1 antibody. Scale bars: 100 μm.

3.5 | Requirement of THG-1 phosphorylation in Ras-mediated tumorigenesis

To investigate the requirement of THG-1 phosphorylation for tumorigenesis, we established HaCaT cells expressing $HRas^{G12V}$, $HRas^{G12V}$-THG-1 (WT), and $HRas^{G12V}$ - THG-1 (S264A) (Figure 5A). We inoculated them into nude mice. As shown in Figure 5B, the tumor growth was significantly promoted in $HRas^{G12V}$-THG-1 (WT) compared with $HRas^{G12V}$. In contrast, THG-1 (S264A) dominantly suppressed $HRas^{G12V}$-mediated tumor formation. Furthermore, the stratified Ki67-positive regions were observed at the edge of $HRas^{G12V}$-THG-1 (WT) tumors. In contrast, a few layered Ki67-positive regions were detected in $HRas^{G12V}$-THG-1 (S264A) tumors (Figure 5C). These results indicated that THG-1 phosphorylation is essential for the enhancement of Ras-mediated tumorigenesis.

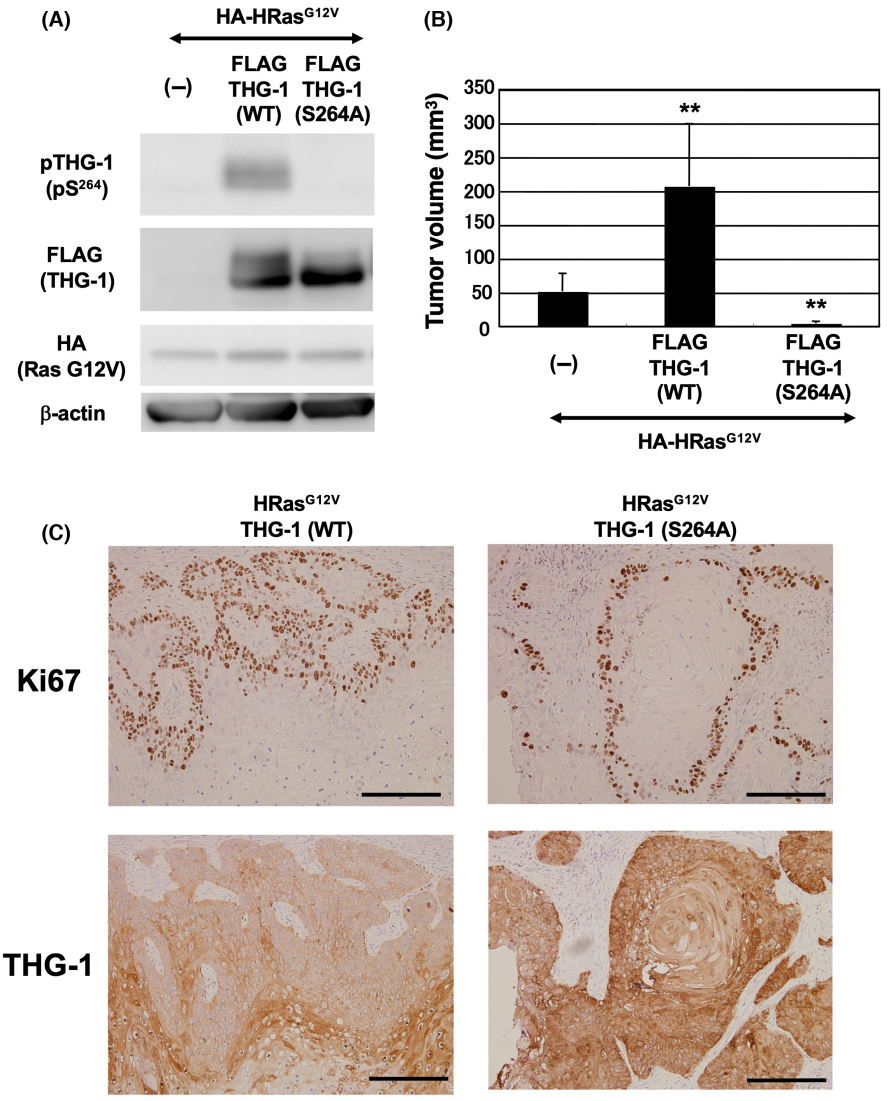

FIGURE 5 Requirement of THG-1 phosphorylation in Ras-mediated tumorigenesis. (A) Anti-phospho-THG-1(pS^{264}) mAb (clone 18), FLAG, HA, and β-Actin immunoblot analyses of HaCaT cells expressing HRas^{G12V}, HRas^{G12V}-THG-1 (WT), and HRas^{G12V}-THG-1 (S264A) (B) Tumor formation in nude mice. Error bars represent means ± SDs. $^{**}p < 0.01$. (C) The sections were stained with anti-THG-1 and Ki67 antibodies. Scale bars: 100 μm.

3.6 | Regulation of EGF-induced CD44 variant inclusion by THG-1

To investigate the THG-1 functions in SCC development in detail, we performed RNA-sequence analysis and found that CD44, an important marker for cancer stem cell and tumor invasiveness, is down-regulated by THG-1 knockdown (Figure S7A). We confirmed that the expression of CD44 was decreased in THG-1-knockdown cells using an anti-pan-CD44 antibody, which recognizes both CD44s and CD44v (Figure 6A). As shown in Figure 6B, CD44s and CD44v are produced by alternative splicing. Using a primer set which amplifies both CD44s and CD44v isoforms (Figure 6B), we performed semi-quantitative RT-PCR to determine the difference of CD44 isoforms in control and the THG-1-knockdown cells. As shown in Figure 6C, the CD44v transcript (~1000 bp) was reduced in THG-1-knockdown cells. Since ERK signaling is known as an inducer of CD44v transcription,[31] we investigated the CD44v transcription in the presence of EGF. EGF stimulation promoted the CD44v transcriptions in control cells, which was not observed in THG-1-knockdown cells (Figure 6D). Furthermore, we sequenced three major bands as shown in Figure 6D and found that they were identified as v3–10, v6–10, and v8–10 isoforms. We next used anti-CD44v9 antibody, which recognizes the variant exon 9-encoded sequence, and confirmed that the induction of CD44v9 by EGF was reduced in THG-1-knockdown cells in flow cytometry (Figure 6E) and immunoblot analysis (Figure S7B). Furthermore, the recovery of CD44v3–10 cDNA into the THG-1-knockdown cell line (TE13 shTHG-1 #2) significantly promoted the sphere-forming ability (Figure 6F,G). These results indicated that the THG-1-CD44v axis is essential to confer the tumorigenic potential to SCC cells.

3.7 | Regulation of CD44 variant splicing by THG-1-knockdown and -overexpressed tumors

We next investigated the CD44 splicing in tumor sphere-forming condition. In THG-1-knockdown cells, we could observe the reduced sphere forming ability in the presence of EGF and bFGF (Figure S8A). In this condition, the CD44v transcription was also reduced in THG-1-knockdown cells (Figure 7A). Furthermore, IHC showed that both

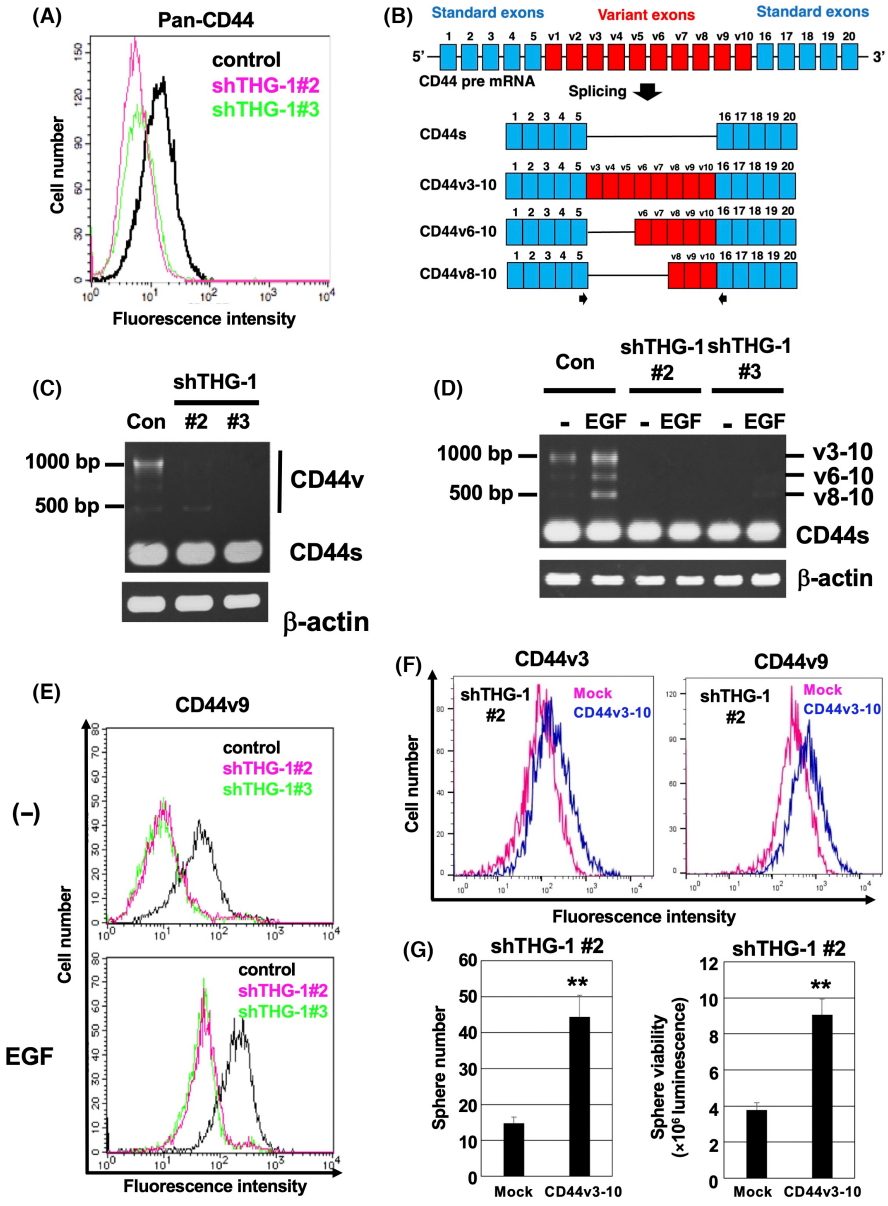

FIGURE 6 Regulation of epidermal growth factor (EGF)-induced CD44 variant splicing by THG-1. (A) Flow cytometry using anti-Pan-CD44 antibody conjugated with PE in TE13 cells expressing shRNAs targeting THG-1 (shTHG-1#2 and shTHG-1#3) or control shRNA. (B) Schematic illustration of CD44s and CD44v. Primers to amplify CD44s and CD44v by semiquantitative RT-PCR are indicated (arrows). (C) Semiquantitative RT-PCR analysis of CD44s and CD44v in control and THG-1-knockdown cells in 10% FBS condition. (D) Semiquantitative RT-PCR analysis of CD44s and CD44v in the presence or absence of 50 ng/mL of EGF (in 0.1% FBS) for 48 h. The indicated bands were identified as CD44v3–10, v6–10, and v8–10 by sequence analysis. (E) Cells were cultured in the presence or absence of 50 ng/mL of EGF (in 0.1% FBS) for 48 h. Flow cytometry was performed by anti-CD44v9 (RV3) antibody. (F) The mock and CD44v3–10-trasfected THG-1-knockdown cells (TE13 shTHG-1 #2) were treated with anti-CD44v3 (C_{44}Mab-6) and anti-CD44v9 (C_{44}Mab-1) antibodies and analyzed using flow cytometry. (G) The sphere number (left) was counted, and the viability (right) was determined using the CellTiter-Glo® 3D Cell Viability Assay in mock and CD44v3–10-trasfected THG-1-knockdown cells. $^{**}p < 0.01$. Error bars represent means ± SDs.

CD44v9 (Figure 7B) and CD44v3 (Figure S8B) were hardly detected in THG-1-knockdown xenograft tumors. As shown in Figure S8C, the THG-1 (WT) could potentiate Ras-mediated tumor sphere formation, but the THG-1 (S264A) could not. In this condition, the transcription of CD44v was elevated in $HRas^{G12V}$-THG-1 (WT)-expressing HaCaT cells (Figure 7C). Furthermore, HaCaT $HRas^{G12V}$-THG-1 (WT) tumors showed an enlarged CD44v9-positive region compared with $HRas^{G12V}$ and $HRas^{G12V}$-THG-1 (S264A) tumors (Figure 7D). These results indicated that the RTK-THG-1 axis is involved in the inclusion of CD44 variant exons.

4 | DISCUSSION

In this study, we provided a novel mechanism of oncogene-induced SCC development through THG-1 phosphorylation. SCCs arise from stratified squamous epithelium and nonsquamous epithelia and have common histological features such as keratin pearls. SCC exhibited resistance to therapy and high invasiveness by potentiating the property of normal squamous epithelium including stratified epithelium formation to protect from stresses[1] and migration during wound closure,[32,33] respectively. In this study, we showed a novel mechanism connecting oncogenic RTK signaling and the SCC tumorigenesis by THG-1. We also showed the involvement of the RTK-THG-1 axis to promote the inclusion of variant exons in CD44 mRNA.

We first revealed the tumor-promoting functions of THG-1. Its knockdown in SCC cells reduced the proliferation, invasiveness, and tumor growth in immunodeficient mice (Figure 2). THG-1 overexpression promoted EGF-induced proliferation, inhibited differentiation during stratified epithelium formation (Figure 3), and potentiated Ras-mediated tumorigenesis through phosphorylation (Figures 4 and 5). We had also performed the knockout of THG-1 in TE13 cells, which exhibited a severe growth retardation

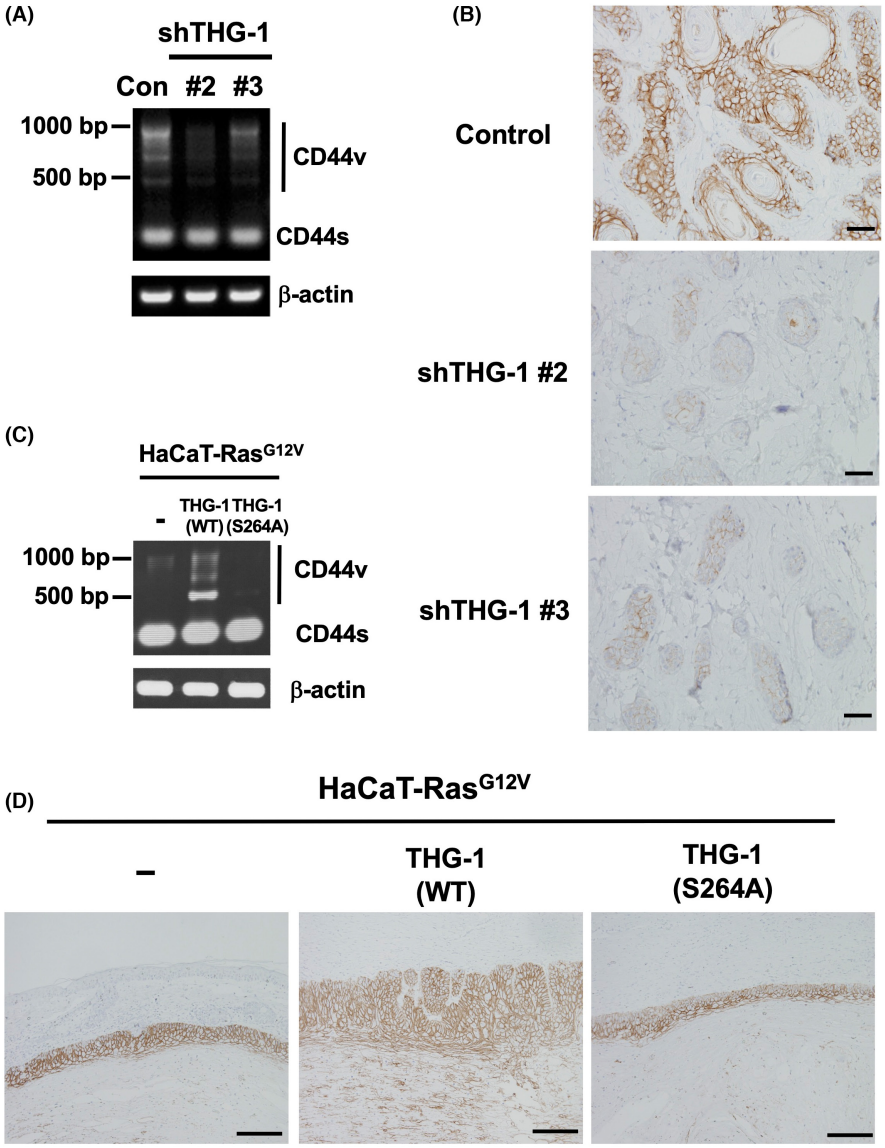

FIGURE 7 Regulation of CD44 variant splicing in THG-1-knockdown and -overexpressed tumors. (A) Decreased CD44v transcription in tumor sphere formation of THG-1-knockdown cells. (B) The xenograft tumor sections in Figure 2E were stained by anti-CD44v9 (RV3) antibody. Scale bars: 100 μm. (C) Increased CD44v transcription in HaCaT-HRas^{G12V}-THG-1 (WT) cells compared with HRas^{G12V}-THG-1 (S264A). (D) The xenograft tumor sections in Figure 5B were stained by anti-CD44v9 (RV3) antibody. Scale bars: 100 μm.

and senescent phenotypes,[34] indicating that THG-1 is essential for tumor proliferation and protects cellular senescence.

Therapeutic strategies against the RTK pathway including anti-RTK mAbs[35] and RTK[36,37]/RAS[38,39]/RAF[40]/MEK[41] inhibitors have been progressively developed, and their clinical trials for SCC have been conducted. We need reliable diagnostic biomarkers to predict the efficacy and prognosis of patients. THG-1 S^{264} is one of the amino acids that is phosphorylated by the RTK-RAS-ERK pathway, which plays crucial roles in RAS-mediated tumorigenesis (Figure 5). The phosphorylation of THG-1 at S^{264} can be detected by established anti-phospho-THG-1(pS^{264}) mAb in IHC (Figure 4F). Therefore, the phosphorylation of THG-1 would be a useful biomarker for diagnosis to determine the sensitivity to RTK-targeted therapy in SCC. Moreover, THG-1 was also detected in gastric SCC (Figure 1C), a rare carcinoma type in stomach. Furthermore, squamous carcinoma or a squamous subtype is also observed in breast[42] and pancreatic carcinomas,[43] which are rare but the most malignant tumors. We have not investigated the expression and phosphorylation of THG-1 in the abovementioned tumors. There is a possibility that THG-1 mediates the malignant property of those carcinomas. Therefore, it could be a future diagnostic marker to be considered.

We showed that THG-1 is a regulator of CD44 splicing (Figure 6) and promotes cell proliferation in the presence of EGF (Figure 3). We found that CD44v expression was decreased in THG-1-knockdown cells (Figure 6) and xenograft tumors (Figure 7). Previously, studies showed that the inclusion of CD44 variant exon is activated by the RAS-RAF-MEK-ERK signaling cascade.[31,44] The Src-associated in mitosis 68 kDa protein (SAM68) enhanced ERK-mediated inclusion of the variant exon 5.[31] Phosphorylated SAM68 bound to the variant exon 5 elements and interacted with SRm160, a splicing activator of pre-mRNAs containing GAA repeats, which was necessary for variant exon 5 inclusion upon Ras activation.[45] We also showed that THG-1 is phosphorylated by the RTK-Ras-ERK pathway, and THG-1 (S264A) mutant could promote neither Ras-mediated tumorigenesis

(Figure 5B) nor CD44v expression (Figure 7C,D). Therefore, phosphorylation of THG-1 is important to induce CD44v expression.

CD44v potentiates RTK signaling as a coreceptor by recruiting FGFs and HB-EGF, which plays critical roles in tumor invasion and stemness.[46] CD44v also plays a critical role in regulation of reactive oxygen species (ROS) defense and tumor growth.[18] CD44v interacts with xCT and controls the intracellular level of reduced glutathione (GSH).[18] In human gastric cancer, a high level of CD44v expression enhanced GSH synthesis and defense against ROS.[18] Furthermore, a selective xCT inhibitor, sulfasalazine, induced apoptosis in CD44v-positive head and neck SCC cells, and treatment of EGFR inhibitor with sulfasalazine resulted in a synergistic reduction of SCC tumor growth.[47] Knockdown of epithelial splicing regulatory protein 1 in CD44v-positive tumor cells results in decreased expression of CD44v, leading to reduced cell surface expression of xCT and suppression of lung metastasis.[48] Since the knockdown of THG-1 also suppressed the abundance of CD44v, the THG-1-CD44v-xCT axis is a potential therapeutic target for the prevention of tumor development.

The detailed molecular mechanism of THG-1 in tumorigenesis should be elucidated in the future studies. We have identified several binding partners of THG-1 using subsequent liquid chromatography–tandem mass spectrometry analyses. These analyses could provide novel insight into the diagnostic and therapeutic strategy against SCC.

AUTHOR CONTRIBUTIONS

All authors have contributed significantly and are in agreement with the content of the manuscript.

ACKNOWLEDGEMENTS

We thank Ms. Yuko Nakayama and Ms. Yoko Miyake for technical assistance.

FUNDING INFORMATION

This work was supported by a JSPS KAKENHI Grant Number 22K06995, 19K07473, and 16K08706 (to H. S.), 22K15596 and 20K16434 (to L. Z), and 17K19580 and 25640059 (to M. K.).

CONFLICT OF INTEREST STATEMENT

The authors have no conflict of interest. Dr. Mitsuyasu Kato is an associate editor of *Cancer Science*.

ETHICS STATEMENT

Approval of the research protocol by an Institutional Review Board: N/A.

Informed consent: N/A.

Registry and the Registration No. of the study/trial: N/A.

Animal studies: Animal experiments were performed with the approval of the Animal Ethics Committee of the University of Tsukuba.

ORCID

Hiroyuki Suzuki https://orcid.org/0000-0003-2646-5132
Yukari Okita https://orcid.org/0000-0002-7279-4634
Yukihide Watanabe https://orcid.org/0000-0003-1014-2910
Yukinari Kato https://orcid.org/0000-0001-5385-8201
Mitsuyasu Kato https://orcid.org/0000-0001-9905-2473

REFERENCES

1. Blanpain C, Fuchs E. Epidermal homeostasis: a balancing act of stem cells in the skin. *Nat Rev Mol Cell Biol*. 2009;10:207-217.
2. Knoblich JA. Asymmetric cell division: recent developments and their implications for tumour biology. *Nat Rev Mol Cell Biol*. 2010;11:849-860.
3. Alam M, Ratner D. Cutaneous squamous-cell carcinoma. *N Engl J Med*. 2001;344:975-983.
4. Rustgi AK, El-Serag HB. Esophageal carcinoma. *N Engl J Med*. 2014;371:2499-2509.
5. Bray F, Loos AH, McCarron P, et al. Trends in cervical squamous cell carcinoma incidence in 13 European countries: changing risk and the effects of screening. *Cancer Epidemiol Biomarkers Prev*. 2005;14:677-686.
6. Leemans CR, Braakhuis BJ, Brakenhoff RH. The molecular biology of head and neck cancer. *Nat Rev Cancer*. 2011;11:9-22.
7. Herbst RS, Heymach JV, Lippman SM. Lung cancer. *N Engl J Med*. 2008;359:1367-1380.
8. Siegel RL, Miller KD, Fuchs HE, Jemal A. Cancer statistics, 2022. *CA Cancer J Clin*. 2022;72:7-33.
9. Dotto GP, Rustgi AK. Squamous cell cancers: a unified perspective on biology and genetics. *Cancer Cell*. 2016;29:622-637.
10. Cancer Genome Atlas Research Network. Comprehensive genomic characterization of squamous cell lung cancers. *Nature*. 2012;489:519-525.
11. Succony L, Rassl DM, Barker AP, McCaughan FM, Rintoul RC. Adenocarcinoma spectrum lesions of the lung: detection, pathology and treatment strategies. *Cancer Treat Rev*. 2021;99:102237.
12. Lin DC, Hao JJ, Nagata Y, et al. Genomic and molecular characterization of esophageal squamous cell carcinoma. *Nat Genet*. 2014;46:467-473.
13. Ponta H, Sherman L, Herrlich PA. CD44: from adhesion molecules to signalling regulators. *Nat Rev Mol Cell Biol*. 2003;4:33-45.
14. Hassn Mesrati M, Syafruddin SE, Mohtar MA, Syahir A. CD44: a multifunctional mediator of cancer progression. *Biomolecules*. 2021;11:1850.
15. Yan Y, Zuo X, Wei D. Concise review: emerging role of CD44 in cancer stem cells: a promising biomarker and therapeutic target. *Stem Cells Transl Med*. 2015;4:1033-1043.
16. Bennett KL, Jackson DG, Simon JC, et al. CD44 isoforms containing exon V3 are responsible for the presentation of heparin-binding growth factor. *J Cell Biol*. 1995;128:687-698.
17. Orian-Rousseau V, Chen L, Sleeman JP, Herrlich P, Ponta H. CD44 is required for two consecutive steps in HGF/c-met signaling. *Genes Dev*. 2002;16:3074-3086.
18. Ishimoto T, Nagano O, Yae T, et al. CD44 variant regulates redox status in cancer cells by stabilizing the xCT subunit of system xc− and thereby promotes tumor growth. *Cancer Cell*. 2011;19:387-400.
19. Guo Q, Yang C, Gao F. The state of CD44 activation in cancer progression and therapeutic targeting. *FEBS J*. 2021;289:7970-7986.
20. Shibanuma M, Kuroki T, Nose K. Isolation of a gene encoding a putative leucine zipper structure that is induced by transforming growth factor beta 1 and other growth factors. *J Biol Chem*. 1992;267:10219-10224.
21. Zheng L, Suzuki H, Nakajo Y, Nakano A, Kato M. Regulation of c-MYC transcriptional activity by transforming growth factor-beta 1-stimulated clone 22. *Cancer Sci*. 2018;109:395-402.
22. Kawamata H, Fujimori T, Imai Y. TSC-22 (TGF-beta stimulated clone-22): a novel molecular target for differentiation-inducing therapy in salivary gland cancer. *Curr Cancer Drug Targets*. 2004;4:521-529.

23. Kester HA, Blanchetot C, den Hertog J, van der Saag PT, van der Burg B. Transforming growth factor-beta-stimulated clone-22 is a member of a family of leucine zipper proteins that can homo- and heterodimerize and has transcriptional repressor activity. *J Biol Chem*. 1999;274:27439-27447.
24. Suzuki H, Kitamura K, Goto N, et al. A novel anti-CD44 variant 3 monoclonal antibody C(44)Mab-6 was established for multiple applications. *Int J Mol Sci*. 2023;24:8411.
25. Tawara M, Suzuki H, Goto N, Tanaka T, Kaneko MK, Kato Y. A novel anti-CD44 variant 9 monoclonal antibody C44Mab-1 was developed for immunohistochemical analyses against colorectal cancers. *Curr Issues Mol Biol*. 2023;45:3658-3673.
26. Kato Y, Kaneko MK, Kuno A, et al. Inhibition of tumor cell-induced platelet aggregation using a novel anti-podoplanin antibody reacting with its platelet-aggregation-stimulating domain. *Biochem Biophys Res Commun*. 2006;349:1301-1307.
27. Fujikura J, Yamato E, Yonemura S, et al. Differentiation of embryonic stem cells is induced by GATA factors. *Genes Dev*. 2002;16:784-789.
28. Asada S, Daitoku H, Matsuzaki H, et al. Mitogen-activated protein kinases, Erk and p38, phosphorylate and regulate Foxo1. *Cell Signal*. 2007;19:519-527.
29. Ikebe D, Wang B, Suzuki H, Kato M. Suppression of keratinocyte stratification by a dominant negative JunB mutant without blocking cell proliferation. *Genes Cells*. 2007;12:197-207.
30. Olsen JV, Blagoev B, Gnad F, et al. Global, in vivo, and site-specific phosphorylation dynamics in signaling networks. *Cell*. 2006;127:635-648.
31. Matter N, Herrlich P, König H. Signal-dependent regulation of splicing via phosphorylation of Sam68. *Nature*. 2002;420:691-695.
32. Shaw TJ, Martin P. Wound repair: a showcase for cell plasticity and migration. *Curr Opin Cell Biol*. 2016;42:29-37.
33. Dekoninck S, Blanpain C. Stem cell dynamics, migration and plasticity during wound healing. *Nat Cell Biol*. 2019;21:18-24.
34. Zhang X, Koga N, Suzuki H, Kato M. Promotion of cellular senescence by THG-1/TSC22D4 knockout through activation of JUNB. *Biochem Biophys Res Commun*. 2020;522:897-902.
35. Kumagai S, Koyama S, Nishikawa H. Antitumour immunity regulated by aberrant ERBB family signalling. *Nat Rev Cancer*. 2021;21:181-197.
36. Cooper AJ, Sequist LV, Lin JJ. Third-generation EGFR and ALK inhibitors: mechanisms of resistance and management. *Nat Rev Clin Oncol*. 2022;19:499-514.
37. Babina IS, Turner NC. Advances and challenges in targeting FGFR signalling in cancer. *Nat Rev Cancer*. 2017;17:318-332.
38. Hallin J, Engstrom LD, Hargis L, et al. The KRAS(G12C) inhibitor MRTX849 provides insight toward therapeutic susceptibility of KRAS-mutant cancers in mouse models and patients. *Cancer Discov*. 2020;10:54-71.
39. Canon J, Rex K, Saiki AY, et al. The clinical KRAS(G12C) inhibitor AMG 510 drives anti-tumour immunity. *Nature*. 2019;575:217-223.
40. Karoulia Z, Gavathiotis E, Poulikakos PI. New perspectives for targeting RAF kinase in human cancer. *Nat Rev Cancer*. 2017;17:676-691.
41. Kim C, Giaccone G. MEK inhibitors under development for treatment of non-small-cell lung cancer. *Expert Opin Investig Drugs*. 2018;27:17-30.
42. Soliman M. Squamous cell carcinoma of the breast: a retrospective study. *J Cancer Res Ther*. 2019;15:1057-1061.
43. Bailey P, Chang DK, Nones K, et al. Genomic analyses identify molecular subtypes of pancreatic cancer. *Nature*. 2016;531:47-52.
44. Weg-Remers S, Ponta H, Herrlich P, König H. Regulation of alternative pre-mRNA splicing by the ERK MAP-kinase pathway. *EMBO J*. 2001;20:4194-4203.
45. Cheng C, Sharp PA. Regulation of CD44 alternative splicing by SRm160 and its potential role in tumor cell invasion. *Mol Cell Biol*. 2006;26:362-370.
46. Zöller M. CD44: can a cancer-initiating cell profit from an abundantly expressed molecule? *Nat Rev Cancer*. 2011;11:254-267.
47. Yoshikawa M, Tsuchihashi K, Ishimoto T, et al. xCT inhibition depletes CD44v-expressing tumor cells that are resistant to EGFR-targeted therapy in head and neck squamous cell carcinoma. *Cancer Res*. 2013;73:1855-1866.
48. Yae T, Tsuchihashi K, Ishimoto T, et al. Alternative splicing of CD44 mRNA by ESRP1 enhances lung colonization of metastatic cancer cell. *Nat Commun*. 2012;3:883.

SUPPORTING INFORMATION

Additional supporting information can be found online in the Supporting Information section at the end of this article.

How to cite this article: Goto N, Suzuki H, Zheng L, et al. Promotion of squamous cell carcinoma tumorigenesis by oncogene-mediated THG-1/TSC22D4 phosphorylation. *Cancer Sci*. 2023;114:3972-3983. doi:10.1111/cas.15934